

# Cobalt Triflates $[\text{Co}(\text{H}_2\text{O})_6](\text{CF}_3\text{SO}_3)_2$ and $\text{Co}(\text{CF}_3\text{SO}_3)_2$ : Synthesis, Crystal Structures, Thermal Stability, and Magnetic Properties

E. V. Karpova<sup>a, \*</sup>, M. A. Ryabov<sup>a</sup>, M. A. Zakharov<sup>a</sup>, A. M. Alekseeva<sup>a</sup>, A. V. Mironov<sup>a</sup>,  
E. S. Kozlyakova<sup>a, b</sup>, V. V. Korolev<sup>b</sup>, and I. V. Morozov<sup>a, b</sup>

<sup>a</sup> Moscow State University, Moscow, Russia

<sup>b</sup> Moscow State Institute of Steel and Alloys (National Research Technological University MISiS), Moscow, Russia

\*e-mail: karpova@inorg.chem.msu.ru

Received February 2, 2022; revised March 15, 2022; accepted March 15, 2022

**Abstract**—Cobalt triflate hexahydrate  $[\text{Co}(\text{H}_2\text{O})_6](\text{CF}_3\text{SO}_3)_2$  (**I**) is crystallized from aquos solution. The dehydration of salt **I** at 200°C in an argon flow affords anhydrous salt  $\text{Co}(\text{CF}_3\text{SO}_3)_2$  (**II**). The crystal structures of compounds **I** and **II** are determined from single crystal and powder X-ray diffraction data, respectively. Compound **I** is isostructural to  $[\text{Ni}(\text{H}_2\text{O})_6](\text{CF}_3\text{SO}_3)_2$  and crystallizes in the space group  $P\bar{3}m1$ ,  $a = 7.3914(16)$ ,  $c = 8.704(2)$  Å,  $V = 411.8(2)$  Å<sup>3</sup>,  $Z = 1$ . The structure of compound **II** (space group  $R\bar{3}$ ,  $a = 4.9996(1)$ ,  $c = 31.3137(8)$  Å,  $V = 677.86(3)$  Å<sup>3</sup>,  $Z = 3$ ) belongs to the structural type  $\text{M}(\text{CF}_3\text{SO}_3)_2$ , where  $\text{M} = \text{Mg, Ca, and Zn}$ . In the structures of both compounds, the cobalt atoms are in the octahedral environment of the oxygen atoms belonging to the water molecules (**I**) or triflate groups (**II**). In compound **I**, the  $[\text{Co}(\text{H}_2\text{O})_6]^{2+}$  cations localized in the nodes of a regular triangular network are linked with the  $(\text{CF}_3\text{SO}_3)^-$  anions via hydrogen bonds to form layers parallel to the (001) plane. When compound **I** is dehydrated to form compound **II**, the  $[\text{CoO}_6]$  octahedra are coupled via the  $\mu_3\text{-CF}_3\text{SO}_3$  group with the retention of the layered structure. The synthesized compounds are characterized by IR spectroscopy, TG/DTA/MS. The results of studying the magnetic properties of compounds **I** and **II** indicate no magnetic ordering at low temperatures and correspond to the paramagnetic behavior of compounds **I** and **II** at high temperatures with a considerable contribution of the spin-orbital interaction to the effective magnetic moment of the cobalt atom.

**Keywords:** cobalt(II) triflates, X-ray diffraction analysis, IR spectroscopy, mass spectrometry, thermal analysis, molecular magnet

**DOI:** 10.1134/S1070328422110057

## INTRODUCTION

Anhydrous triflates exhibit the properties of Lewis acids and are used as catalysts in diverse organic reactions. Trifluoromethanesulfonic acid  $\text{CF}_3\text{SO}_3\text{H}$  and its salts, trifluoromethanesulfonates (triflates), find wide use in nucleophilic substitution reactions. For example, methyl and ethyl triflates are more reactive by approximately 25000 times than the corresponding tosylates, and the hydrolysis of ethyl triflate is an  $\text{S}_{\text{N}}2$  process [1]. Interest in triflates is due not only to their use as catalysts. Many triflates remain poorly studied up to presently, including lacking data on their crystal structures and thermal stability. In addition, the study of the magnetic properties of triflates is of certain interest, which is due to a possibility of accomplishing low-dimensional magnetic ordering or geometry-conditioned frustration [2]. The present published data on the crystal structures of *d*-element triflates are rather restricted. For instance, the data are available on the structures of some *3d*-metal triflate hexahydrates  $\text{M}(\text{CF}_3\text{SO}_3)_2 \cdot 6\text{H}_2\text{O}$ , where  $\text{M} = \text{Fe}$  [3] and  $\text{Ni}$  [4],

and only an information about the synthesis and some properties of triflate heptahydrate  $[\text{Co}(\text{H}_2\text{O})_6](\text{CF}_3\text{SO}_3)_2 \cdot \text{H}_2\text{O}$  is published [5]. There are also data on the structures of several triflates of divalent metals  $\text{M}(\text{CF}_3\text{SO}_3)_2$ , where  $\text{M} = \text{Mg, Ca, Ba, Zn, and Cu}$  [6] and properties of anhydrous triflate  $\text{Co}(\text{CF}_3\text{SO}_3)_2$  [5, 7]. In this work, we present the synthesis and crystal structures of cobalt triflate hexahydrate  $[\text{Co}(\text{H}_2\text{O})_6](\text{CF}_3\text{SO}_3)_2$  (**I**) and anhydrous triflate  $\text{Co}(\text{CF}_3\text{SO}_3)_2$  (**II**). The synthesized compounds were characterized by IR spectroscopy, and their thermal stability and magnetic properties were studied.

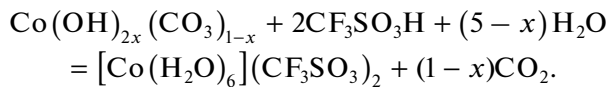
## EXPERIMENTAL

Trifluoromethanesulfonic acid ( $\text{CF}_3\text{SO}_3\text{H}$ , 99%, extra pure, ACROS), basic cobalt carbonate  $\text{Co}(\text{OH})_{2x}(\text{CO}_3)_{1-x}$  (analytical grade), and distilled water were used.

Samples of compound **I** were stored under the mother liquor in sealed weighing bottles or as crystal-

line samples in sealed weighing bottles. Samples of compound **II** were stored in a glove box of the trade mark "Spectroscopic systems" with a controlled argon atmosphere ( $p(\text{O}_2), p(\text{H}_2\text{O}) < 0.1 \text{ ppm}$ ).

**Synthesis of  $[\text{Co}(\text{H}_2\text{O})_6](\text{CF}_3\text{SO}_3)_2$  (I).** Compound **I** was synthesized by the gradual concentrating of an aqueous solution prepared by the dissolution of basic cobalt(II) carbonate in 30% trifluoromethanesulfonic acid as follows:



A red-orange solution is formed due to the interaction of the starting substances (regardless of their ratio). The storage of the solution at room temperature in air for 7 days results in the crystallization of orange-red rhombohedral crystals of compound **I**.

IR for **I** ( $\nu, \text{cm}^{-1}$ ): 3600–3200  $\nu(\text{OH})$ , 1648, 1615  $\delta(\text{OH})$ , 1229, 1187  $\nu(\text{CF}_3)$ ,  $\nu_{\text{as}}(\text{SO}_3)$ , 1028  $\nu_{\text{s}}(\text{SO}_3)$ , 767, 719  $\nu(\text{C–S})$ ,  $\delta_{\text{s}}(\text{CF}_3)$ , 633  $\delta_{\text{as}}(\text{SO}_3)$  [7, 8].

**Synthesis of  $\text{Co}(\text{CF}_3\text{SO}_3)_2$  (II).** Conditions for the synthesis of compound **II** were chosen on the basis of the thermal analysis results. A polycrystalline single-phase sample of compound **II** was obtained due to holding compound **I** in a platinum crucible at 200°C in an argon flow for 3 h. To prevent the interaction of compound **II** with water vapors, all synthetic procedures and sample storage were carried out under an inert atmosphere, and a scotch amorphous to X rays was used in X-ray diffraction (XRD) studies.

IR spectra were recorded on a Perkin Elmer Spectrum One spectrometer equipped with an attenuated total reflectance (ATR) accessory for recording in the wavenumber range from 580 to 4000  $\text{cm}^{-1}$ .

Thermogravimetric analysis (TG), differential thermal analysis (DTA), and mass spectrometry (MS) of gaseous decomposition products were carried out on a NETZSCH STA409 PC/PG analyzer equipped with a NETZSCH QMS403C quadrupole mass analyzer in an argon flow using a gas flow rate of 20 mL/min and a heating rate of 5°C/min in the temperature range from 20 to 800°C.

A polycrystalline sample of compound **I** was studied by the synchrotron radiation X-ray powder diffraction technique ( $\lambda = 0.35451 \text{ \AA}$ ,  $T = 200 \text{ K}$ ) (European Synchrotron Radiation Facility (ESRF), ID22, Grenoble, France).

The XRD powder data for compound **II** were obtained at room temperature using a high-resolution Guinier camera (Image Plate Huber G670,  $\text{Co}K_{\alpha}$  radiation,  $\lambda = 1.79028 \text{ \AA}$ , Ge(111) monochromator, angle range 3.000–100.300  $2\theta^{\circ}$ , increment 0.005). Under an inert atmosphere, the samples pretriturated in an agate mortar were deposited on a lavsan film amorphous to X rays and immobilized on a cassette of the diffractometer with the Kapton® scotch am-

phous to X rays. Some samples were studied using a Rigaku D/MAX 2500 diffractometer (reflection geometry,  $\text{Cu}K_{\alpha}$  radiation,  $\lambda = 1.540598 \text{ \AA}$ , graphite monochromator).

The PDF-2+ databases [9] and the STOE WinXPow [10] and JANA2006 [11] program packages were used for XRD powder data processing.

Additional data on the crystal structure of compound **II** are available at the Fachinformationszentrum Karlsruhe database (ICSD no. 2141865; crys-data@fiz-karlsruhe.de).

**XRD** of compound **I** was carried out on a STOE StadiVari Pilatus 100 K diffractometer ( $\text{Cu}K_{\alpha}$  radiation,  $\lambda = 1.54186 \text{ \AA}$ ). Structural data were processed and examined during structure solution and refinement in the WinGX program shell [12]. An absorption correction was applied analytically taking into account an uncertain shape of the crystal used for structural experiments. The measured reflection intensities were corrected to the Lorentz and polarization factors. The structure of compound **I** was solved using the SHELXT program [13]. Cobalt, sulfur, and oxygen atoms were found initially. Carbon, fluorine, and hydrogen atoms were determined from the difference Fourier syntheses. The positions of non-hydrogen atoms were refined anisotropically, and those of hydrogen atoms were refined isotropically in the full-matrix approximation using the SHELXL program [14]. The crystallographic data and parameters of the XRD single-crystal experiment for compound **I** are given in Table 1. Selected interatomic distances for the structure of compound **I** are listed in Table 2 [4, 5].

Additional data on the crystal structure of compound **I** are available at the Fachinformationszentrum Karlsruhe database (ICSD no. 1941425; crys-data@fiz-karlsruhe.de).

The temperature ( $\chi(T)$ ) and field ( $M(B)$ ) dependences of the magnetization at 2–300 K and 0–9 T, respectively, were measured on an MPMS-XL7 SQUID magnetometer (Magnetic Property Measurement System, Quantum Design) and a vibromagnetometer implemented in the Physical Property Measurement System (PPMS, Quantum Design). To prevent a change in the hydrate composition of the samples, they were stored and measured in sealed glass ampules under an argon atmosphere. The weight of the measured samples ranged from 15 to 25 mg.

## RESULTS AND DISCUSSION

A polycrystalline sample of compound **I** prepared by the trituration of the crystals was studied by the synchrotron radiation X-ray powder diffraction technique at 200 K. The positions and relative intensities of reflections on the X-ray pattern of compound **I** resemble those for nickel triflate hexahydrate  $[\text{Ni}(\text{H}_2\text{O})_6](\text{CF}_3\text{SO}_3)_2$  [4] (Fig. 1). Such a similarity suggests the formation of an isostructural compound

**Table 1.** Crystallographic data and structure refinement parameters for compound **I**

Parameter	Value
Empirical formula	$\text{C}_2\text{H}_{12}\text{O}_{12}\text{F}_6\text{S}_2\text{Co}$
Space group	$P\bar{3}m1$ (no. 164)
$a$ , Å	7.3914(16)
$c$ , Å	8.704(2)
$V$ , Å <sup>3</sup>	411.8(2)
$Z$	1
$\rho_{\text{calc}}$ , g cm <sup>-3</sup>	1.876
Radiation ( $\lambda$ , Å)	$\text{Cu}K_{\alpha}$ (1.54186)
Range of $h$ , $k$ , $l$	$-8 \leq h \leq 7; -1 \leq k \leq 8; -10 \leq l \leq 10$
Range of $2\theta$ , deg	5.08–66.13
$T$ , K	293(2)
$\mu$ , cm <sup>-1</sup>	11.695
Number of reflections collected/independent/ $I > 2\sigma(I)$	2358/307/197
$R_{\text{int}}$	0.056
Number of refined parameters	31
Data completeness, %	98.1
GOOF	0.996
$R_1$	0.049
$wR_2$ ( $I \geq 2\sigma(I)$ )	0.110
Residual electron density (max/min), e Å <sup>-3</sup>	0.301/–0.419

**Table 2.** Interatomic distances (Å) in the structures of compounds **I** and **II** compared with the isostructural analogs  $[\text{Ni}(\text{H}_2\text{O})_6](\text{CF}_3\text{SO}_3)_2$  [4] and  $\text{Zn}(\text{CF}_3\text{SO}_3)_2$  [6]

Bond	$[\text{Co}(\text{H}_2\text{O})_6](\text{CF}_3\text{SO}_3)_2^*$	$[\text{Ni}(\text{H}_2\text{O})_6](\text{CF}_3\text{SO}_3)_2$	$\text{Co}(\text{CF}_3\text{SO}_3)_2^*$	$\text{Zn}(\text{CF}_3\text{SO}_3)_2$
M–O	2.074(5)	2.035(2)	2.032(1)	2.069(2)
S–O	1.447(4)	1.443(2)	1.508(2)	1.445(3)
C–S	1.809(15)	1.830(6)	1.758(5)	1.820(2)
C–F	1.321(6)	1.322(3)	1.376(2)	1.302(3)

\* This work.

$[\text{Co}(\text{H}_2\text{O})_6](\text{CF}_3\text{SO}_3)_2$  (**I**). All reflections on the pattern were indexed in the trigonal crystal system (space group  $P\bar{3}m1$ ) with the unit cell parameters  $a = 7.3592(2)$ ,  $c = 8.72103(4)$  Å,  $R_p = 0.106$ .

A regular increase in the unit cell parameters compared to  $[\text{Ni}(\text{H}_2\text{O})_6](\text{CF}_3\text{SO}_3)_2$  ( $a = 7.368(3)$ ,  $c = 8.672(4)$  Å [4]) is attributed to an increase in the ion radius of the  $\text{Co}^{2+}$  cation (high-spin state, coordination number 6:  $r(\text{Co}^{2+}) = 0.745$  Å,  $r(\text{Ni}^{2+}) = 0.69$  Å).

The IR spectrum of compound **I** correlates with that of anhydrous cobalt triflate [15], and the bands were assigned according to published data [8]. As compared to the data for the anhydrous salt [15], the appearance of a broad peak in a range of 3200–

3600 cm<sup>-1</sup> in the IR spectrum indicates the presence of water of crystallization. The symmetric vibration band  $\nu_{\text{as}}(\text{SO}_3)$  is shifted to the short-wavelength range, which is possibly associated with different coordination modes of the triflate anion as in [5, 7].

The TG and DTA analyses combined with the MS analysis of the gaseous decomposition products showed that compound **I** decomposed in two stages (Fig. 2). The first stage (dehydration) starts immediately after the heating onset and ceases at 135°C. A plateau is reached after the loss of 22.77% initial mass, which corresponds to the removal of all the water of crystallization and formation of anhydrous salt **II** via the following reaction (theoretical mass loss 23.2%):

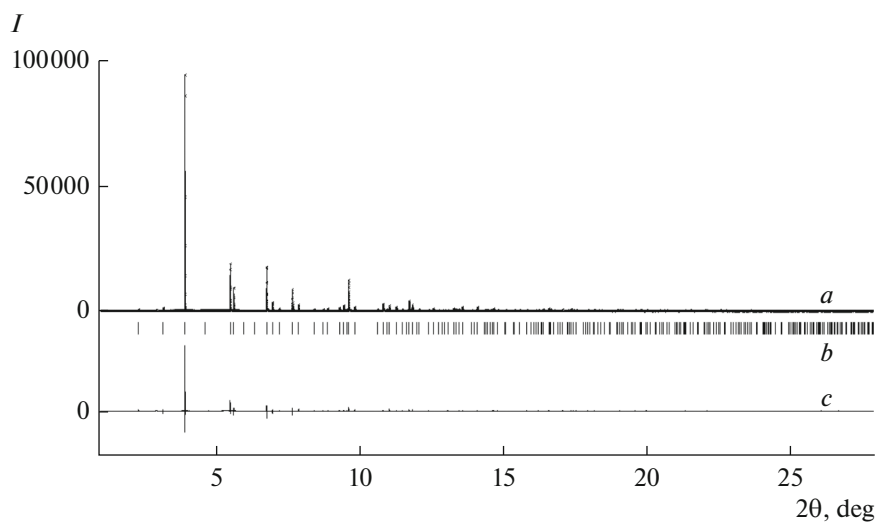
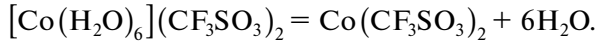


**Fig. 1.** (a) Experimental, (b) calculated, and (c) difference XRD patterns of  $[\text{Co}(\text{H}_2\text{O})_6](\text{CF}_3\text{SO}_3)_2$  obtained in the synchrotron radiation ( $\lambda = 0.35451 \text{ \AA}$ , 200 K).



According to the TG data, compound **II** is stable in a wide temperature range up to 460°C. A temperature range of 460–520°C exhibits a sharp mass loss equal to 55.93 wt % of the initial mass, which corresponds well to the formation of  $\text{CoF}_2$  (theoretical mass loss 55.91%), and no formation of water molecules is observed. The XRD powder data for the sample after TG analysis confirm the formation of cobalt fluoride  $\text{CoF}_2$ . Thus, at temperatures above 460°C compound **II** decomposes to form  $\text{CoF}_2$  (Fig. 3) [16].

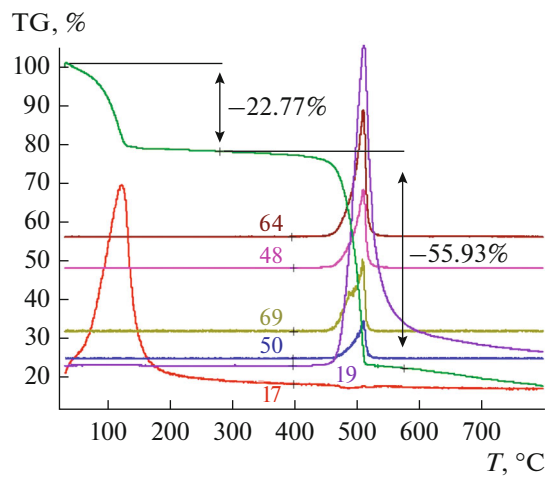


**Fig. 2.** Thermogravimetric (TG) dependence of a change in the relative weight and the main ion currents in the mass spectrum (MS) of the gaseous decomposition products for sample I (mass numbers of the corresponding ion currents are presented).

The XRD pattern of the obtained sample of compound **II** is shown in Fig. 4. All reflections on the pattern were indexed in the hexagonal crystal system with the parameters  $a = 4.9996(1)$ ,  $c = 31.3137(8) \text{ \AA}$ . The systematic reflection quenchings ( $hkl: -h + k + l = 3n$ ) correspond to the space group  $R\bar{3}$  characteristic of anhydrous triflates of doubly charged cations  $\text{M}(\text{CF}_3\text{SO}_3)_2$ , where  $\text{M} = \text{Mg, Ca, and Zn}$  [6]. It should be mentioned that compound **II** is extremely hygroscopic: even a short contact of compound **II** with air led to the appearance of an impurity of crystalline hydrate **I**.

The structure of compound **I** (Fig. 5) consists of layers formed by the  $[\text{Co}(\text{H}_2\text{O})_6]$  octahedra and

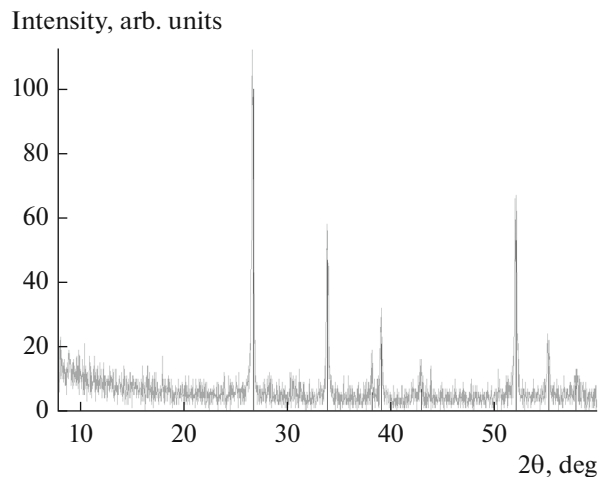


**Fig. 3.** Comparison of the XRD pattern of the crystalline product of the decomposition of sample **II** with the theoretical XRD pattern of  $\text{CoF}_2$  (bar XRD pattern) [16].

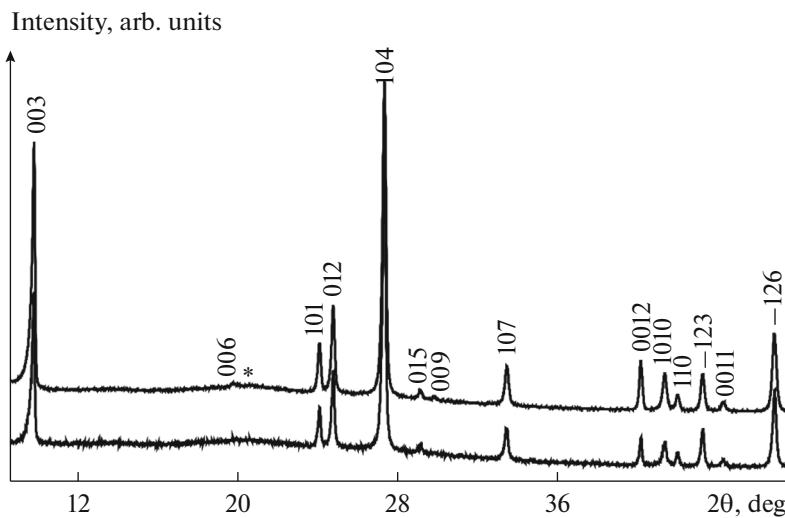


**Fig. 4.** Region of the XRD patterns of sample **II** ( $\text{CoK}_\alpha$  radiation). Upper XRD pattern was obtained in a longer XRD experiment. Sign \* marks the reflection of an impurity of compound **I**. Reflection indices correspond to the hexagonal cell with the parameters  $a = 4.9996(1)$ ,  $c = 31.3137(8)$  Å.

$(\text{CF}_3\text{SO}_3)$  triflate groups arranged along the [001] direction. The octahedra contain six equal Co–O contacts linking the cobalt atom with the oxygen atoms of the water molecules. The layers are formed due to hydrogen bonds formed by the hydrogen atoms of the water molecules and oxygen atoms of the triflate group ( $\text{O}_\text{w}–\text{H}$  0.87(5),  $\text{H}... \text{O}$  1.98(5),  $\text{O}_\text{w}... \text{O}$  2.817(4) Å,  $\text{O}_\text{w}–\text{H}... \text{O}$  161°).

In the layers parallel to the (001) plane, the  $[\text{Co}(\text{H}_2\text{O})_6]$  octahedra are arranged according to the regular triangular network motif (Fig. 6, *a*). The  $\text{CF}_3$  groups are directed to the interlayer space in such a way that the minimum distance in the (001) plane between the fluorine atoms from the adjacent layers is 3.045 Å.

The structure of compound **II** was refined by the Rietveld method according to the XRD powder data using the structure of  $\text{Zn}(\text{CF}_3\text{SO}_3)_2$  [6] as the starting model. The crystallographic data and parameters of the XRD powder experiment for compound **II** are given in Table 3. Selected interatomic distances are listed in Table 2. The experimental, calculated, and difference XRD patterns are shown in Fig. 6.

It should be mentioned that the structures of compounds  $\text{M}(\text{CF}_3\text{SO}_3)_2$ , where  $\text{M} = \text{Mg}$ ,  $\text{Ca}$ , and  $\text{Zn}$ , were solved [6] using the synchrotron radiation X-ray powder diffraction data. The disordering of the O and F atoms (arranged at distances shorter than 0.05 Å from each other) over three positions with fixed occupancy of 0.333 was introduced into the structural model. The structural model with one crystallographically independent position of O and one position of F was used in this work. The O atom is included in the first coordination sphere of cobalt, which makes its disordering poorly probable. The situation with a pos-

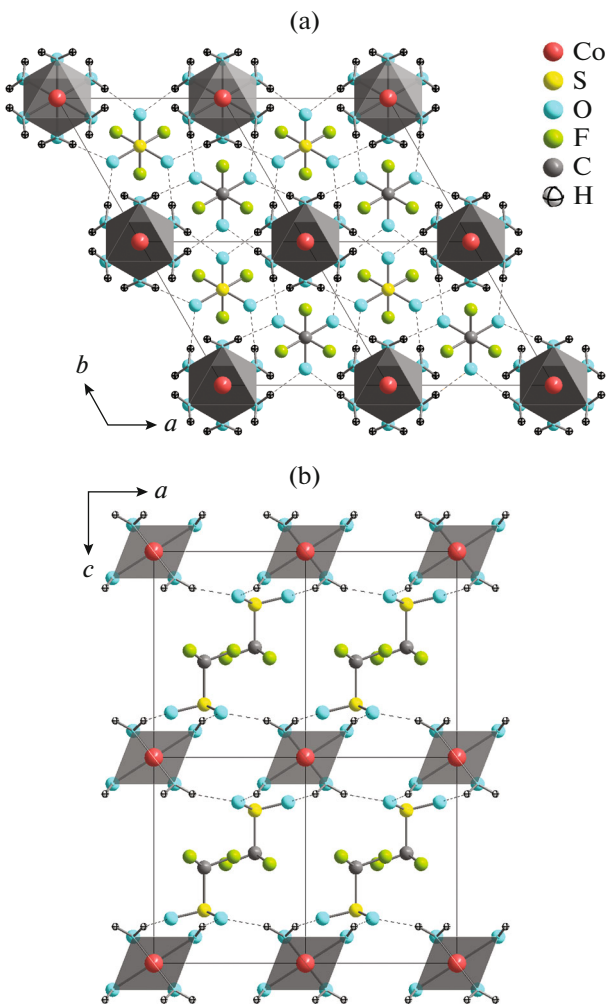


**Fig. 5.** Structure of  $[\text{Co}(\text{H}_2\text{O})_6](\text{CF}_3\text{SO}_3)_2$ : views along the (a)  $c$  and (b)  $b$  axes.

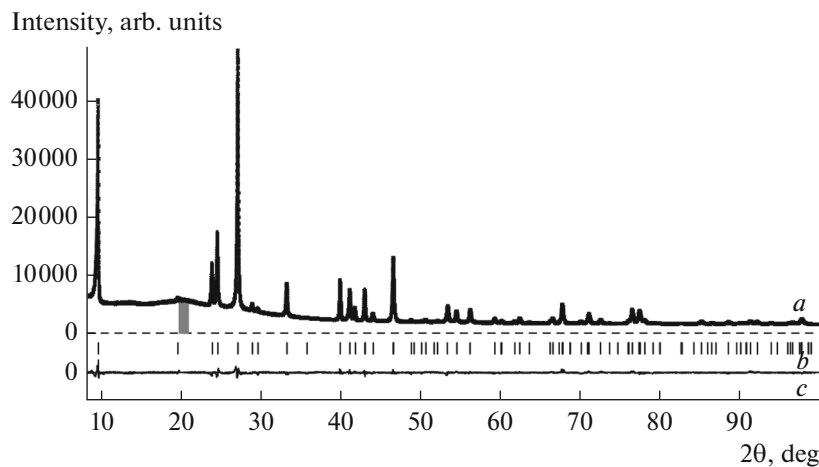


**Fig. 6.** (a) Experimental, (b) calculated, and (c) difference XRD patterns of the structure of compound **II** refined by the Rietveld method. The region (gray) corresponding to an impurity of compound **I** formed with an increased time of an XRD experiment was excluded from refinement.

sible disordering of the  $\text{CF}_3$  groups is much more complicated. These groups of the adjacent layers in the structure of compound **I** lie in one plane creating steric hindrances for their free rotation, whereas the  $\text{CF}_3$  groups in the structure of compound **II** are completely separated (the separation width can be estimated as 2.71 Å), which assumes a possibility of free rotation. A similar rotation is known even for larger fragments of

**Table 3.** Crystallographic data and selected parameters of the XRD powder experiment for compound **II**

Parameter	Value
Empirical formula	$\text{C}_2\text{O}_6\text{F}_6\text{S}_2\text{Co}$
$FW$	357.1
Space group	$R\bar{3}$ (no. 148)
$a$ , Å	4.9996(1)
$c$ , Å	31.3137(8)
$V$ , Å <sup>3</sup>	677.86(3)
$Z$	3
$\rho_{\text{calc}}$ , g cm <sup>-3</sup>	2.62
Radiation ( $\lambda$ , Å)	$\text{Co}K_{\alpha}/1.79028$
Range of $2\theta$ , deg	8.440–100.005
$T$ , K	295
$\mu$ , cm <sup>-1</sup>	12.89
Number of points	18313
Number of observed reflections	105
Number of refined parameters	31
$R_{\text{I}}$ , $R_{\text{exp}}$	0.0603, 0.0179
$R_{\text{p}}$ , $R_{\text{wp}}$	0.022, 0.030
GOF	1.66

molecules, such as methylated cyclopentadienyl [17]. Several preferable positions of the  $\text{CF}_3$  groups in the structure of  $\text{Co}(\text{CF}_3\text{SO}_3)_2$  are most probable, but they cannot be determined using laboratory powder diffraction data. Therefore, in this work we restricted our consideration by the structural model with one independent position of the F atom.

The dehydration of compound **I** with the formation of compound **II** is accompanied by the retention of the layered structure due to binding the  $[\text{CoO}_6]$  octahedra by the  $\mu_3$ -( $\text{CF}_3\text{SO}_3$ ) groups (Fig. 7). The triangular motif of  $\text{Co}^{2+}$  cation arrangement is retained.

The structure of compound **II** as compared to compound **I** exhibits a regular insignificant shortening of the Co–O distance (Table 2) together with a substantial (from ~7.4 to ~5 Å) shortening of the distance between the adjacent  $[\text{CoO}_6]/(\text{CF}_3\text{SO}_3)$  groups in the layer. This results in the displacement of the layers relative to each other along the [001] direction by (1/3, 1/3, 0) and trebling of the  $c$  parameter. In the structure of compound **II**, the  $\text{CF}_3$  groups are separated with a cavity, whereas the F atoms of the adjacent layers in compound **I** lie nearly in one plane.

The behavior of the temperature dependences of the magnetic susceptibility ( $\chi(T)$ ) for compounds **I** and **II** (Fig. 8) can be described by the Curie–Weiss law  $\chi = \chi_0 + \frac{C_{\text{CW}}}{T - \Theta}$  in a wide temperature range of 15–300 K for compound **I** and of 90–300 K for compound **II**. The temperature dependences  $\chi(T)$  (Fig. 8a) for compounds **I** and **II** were measured in the field  $B = 0.1$  T. The dependences of the inverse susceptibility  $1/(\chi - \chi_0)$  are shown in Fig. 8a (inset) and demonstrate a linear behavior at high temperatures according to the Curie–Weiss law and a deviation from linearity at low temperatures, which possibly

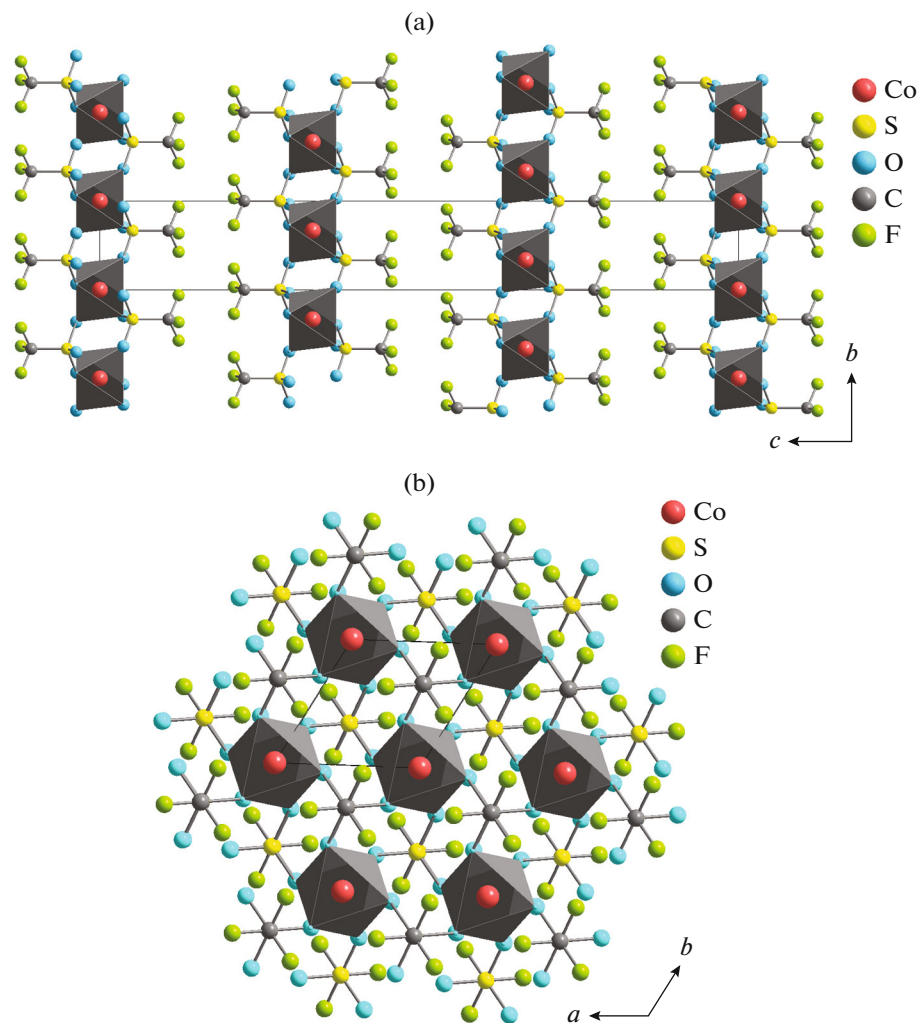


**Fig. 7.** Structure of  $\text{Co}(\text{CF}_3\text{SO}_3)_2$ : views along the (a)  $a$  and (b)  $c$  axes (atoms of one layer).

indicates a contribution of effects of the spin-orbit interaction of the cobalt ions and crystalline field effects. The  $M(B)$  dependences for compounds **I** and **II** measured at 2 and 300 K are shown in Fig. 8b.

No features of long-range magnetic order are observed for cobalt triflates at low temperatures. The data on  $\chi(T)$  and  $M(B)$  obtained for both samples qualitatively correspond to the paramagnetic behavior in the whole temperature range studied (2–300 K) with a considerable contribution of the spin-orbit interaction to the magnetic properties. The low-temperature dependences  $M(B)$  were described by the sum of the Brillouin function and a linear contribution presumably corresponding to the Van Vleck paramagnetism [18] as follows:

$$M(B) = Ng_J\mu_B J \left[ \frac{2J+1}{2J} \cosh \left( \frac{2J+1}{2J} \frac{g_J\mu_B J B}{k_B T} \right) - \frac{1}{2J} \cosh \left( \frac{1}{2J} \frac{g_J\mu_B J B}{k_B T} \right) \right] + \chi_0 B.$$

For compound **I**, the optimum  $g$  factor was 3.32 and the full angular moment ( $J$ ) was 0.72 at 2 K. For anhydrous salt **II**, the  $g$  factor is 3.84 and  $J$  is close to the theoretical value equal to  $1/2$ . So high  $g$  factors correspond to the literature data for  $\text{Co}^{2+}$  in the octahedral environment [19]. It is also well known for the cobalt compounds that the full angular moment is close to  $J = 1/2$ , which differs from the spin-only value  $S = 3/2$ .

The deviation from the Curie–Weiss law can be due to a contribution of exchange interactions of the short-range order, the spin-orbit interaction, or a contribution of defects/impurities. The negative Weiss constants  $\theta \approx -5.6$  K for compound **I** and  $\theta \approx -54$  K for compound **II** show that the antiferromagnetic exchange interaction prevails in the magnetic subsystem. The Curie constants  $C_{\text{CW}} \approx 2.53$  emu/(mol K) for compound **I** and  $C_{\text{CW}} \approx 3.96$  emu/(mol K) for compound **II** give the estimate of the effective magnetic moment ( $\mu_{\text{eff}}$ ) equal to 4.5 and 5.6  $\mu_B$ , respectively.

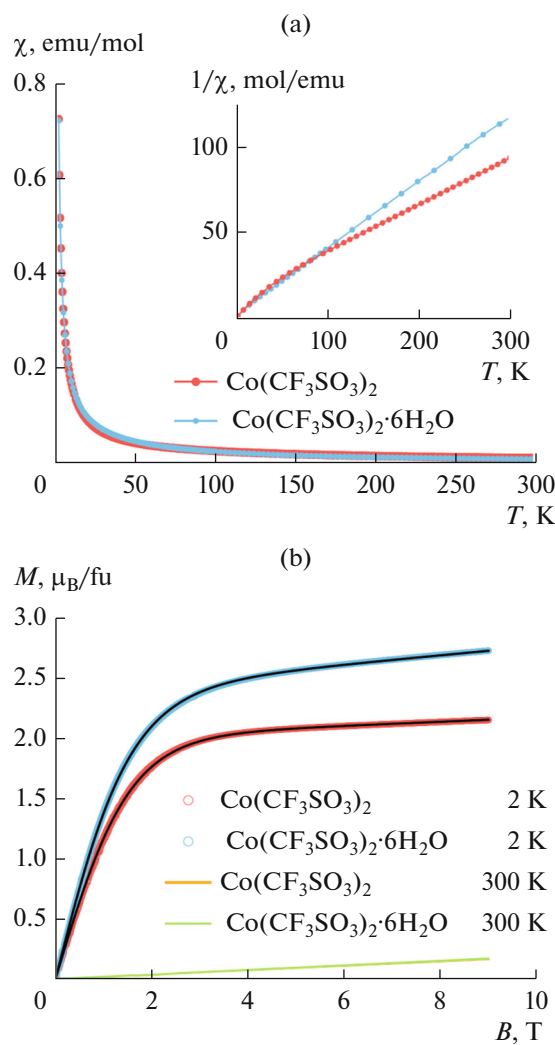


**Fig. 8.** (a) Temperature dependences of the magnetic susceptibility  $\chi(T)$  for compounds **I** (blue) and **II** (red) measured in the cooling mode in the field (FC)  $B = 0.1$  T (inset: dependences of the inverse susceptibility  $(\chi - \chi_0)^{-1}(T)$ ) and (b) the field dependences of the susceptibility for compounds **I** and **II** measured at 2 and 300 K (approximation of the experimental curves by the Brillouin function is shown by black lines).

These values substantially exceed the theoretical spin-only value for high-spin  $\text{Co}^{2+}$  with  $S = 3/2$  ( $\mu_{\text{eff}} = 2\sqrt{S(S+1)} = 3.87 \mu_B$ ). This indicates a significant contribution of the spin-orbit interaction to the magnetic moment, which corresponds to the data of the  $M(B)$  field dependences. A comparison with the published data [5] demonstrates a similarity of the obtained values. The value of  $\mu_{\text{eff}}$  for the hydrate is somewhat higher and equals  $4.87 \mu_B$ , which can be due to impurities or to the fact that this characteristic is presented for the compound with a different composition:  $\text{Co}(\text{CF}_3\text{SO}_3)_2 \cdot 7\text{H}_2\text{O}$ . The magnetic moment for the anhydrous salt is somewhat lower than that deter-

mined by us and equals  $5.31 \mu_B$ , which can be related to an impurity of crystalline hydrate.

Our data for compound **I**, including quantitative results, show a similarity with the known molecular magnets based on  $\text{Co}(\text{II})$  ions in the octahedral environment of the ligands. A similar behavior of  $\chi(T)$  and  $M(B)$  was observed for a square magnetic 2D lattice of  $\text{Co}(\text{II})$  [20],  $\text{Co}(\text{II})$ -based molecular clusters of various dimensionalities [21], and a triangular magnetic 2D sublattice of  $\text{Co}(\text{OH})_2$  [22] and corresponds to the theoretical concepts on the behavior of the  $\text{Co}(\text{II})$ -based molecular magnets [23]. At the same time, a fairly high Weiss temperature  $\theta = -54$  K for compound **II** indicates a sufficiently strong magnetic exchange interaction between the cobalt ions, which can approximately be estimated by the equation  $\sum J \approx 3\theta/(S(S+1)) \approx -43$  K. The absence of magnetic ordering properties down to low temperatures (2 K) and the triangular motif of the cobalt ions in the structure indicate that the frustration of exchange interactions can strongly contribute to the magnetic properties of this compound. However, it should be kept in mind that a similar pattern can be provided by a strong contribution from the spin-orbit interaction thus violating the obtained Weiss temperatures. The first-principles calculations of the magnetic subsystem of cobalt triflates with allowance for the spin-orbit interactions should be performed for a more precise description of the magnetic subsystem.

#### ACKNOWLEDGMENTS

This work was carried out using equipment purchased due to facilities of the program for the development of the Moscow State University

#### FUNDING

This work was supported by the Russian Foundation for Basic Research, project no. 19-03-01059.

#### CONFLICT OF INTEREST

The authors declare that they have no conflicts of interest.

#### REFERENCES

1. Su, T.M., Sliwinski, W.F., and Schleyer, P.V.R., *J. Am. Chem. Soc.*, 1969, vol. 91, no. 19, p. 5386.
2. Vasil'ev, A.N., Volkova, O.S., Zvereva, E.A., et al., *Nizkorazmernyi magnetizm* (Low-Dimensional Magnetism), Moscow: Fizmatlit, 2018.
3. Kaduk, J.A., *Powder Diffr.*, 1999, vol. 14, no. 3, p. 166.
4. Sidorov, A.A., Reshetnikov, A.V., Deomidov, S.M., et al., *Zh. Neorg. Khim.*, 2000, vol. 45, p. 793.
5. Jansky, M.T. and Yoke, J.T., *J. Inorg. Nucl. Chem.*, 1979, vol. 41, no. 12, p. 1707.

6. Dinnebier, R., Sofina, N., Hildebrandt, L., et al., *Acta Crystallogr., Sect. B: Struct. Sci.*, 2006, vol. 62, no. 3, p. 467.
7. Boumizane, K., Herzog-Cance, M.H., Jones, D.J., et al., *Polyhedron*, 1991, vol. 10, nos. 23–24, p. 2757.
8. Socrates, G., *Infrared and Raman Characteristic Group Frequencies: Tables and Charts*, Chichester: Wiley, 2004.
9. *ICDD PDF-2+ (Database)*, International Centre for Diffraction Data: Newtown Square, 1998.
10. *WinXPOW D.S. Version 2.21*, Darmstadt: Stoe & Cie GmbH, 2007.
11. Petříček, V., Dušek, M., and Palatinus, L., *Z. Kristallogr. Cryst. Mater.*, 2014, vol. 229, no. 5, p. 345.
12. Farrugia, L.J. *J. Appl. Crystallogr.*, 1999, vol. 32, p. 837.
13. Sheldrick, G.M., *Acta Crystallogr., Sect. A: Found. Adv.*, 2015, vol. 71, p. 3.
14. Sheldrick, G.M., *Acta Crystallogr., Sect. C: Struct. Chem.*, 2015, vol. 71, p. 3.
15. Arduini, A.L., Garnett, M., Thompson, R.C., et al., *Can. J. Chem.*, 1975, vol. 53, no. 24, p. 3812.
16. ICDD PDF-2 (Database), International Centre for Diffraction Data: Newtown Square. nos. 00-024-0329, 071-0653, 081-2033.
17. Kudinov, A.R., Muratov, D.V., Rybinskaya, M.I., et al., *J. Organomet. Chem.*, 1991, vol. 414, p. 97.
18. Blundell, S., *Magnetism in Condensed Matter*, Oxford: Master Series in Physics, Oxford University, 2001, p. 29.
19. Piwowarska, D., Gnutek, P., and Rudowicz, C., *Appl. Magn. Reson.*, 2019, vol. 50, p. 797.
20. Tiwari, A., Bhosle, V.M., Ramachandran, S., et al., *Appl. Phys. Lett.*, 2006, vol. 88, no. 14, p. 142511.
21. Murrie, M., *Chem. Soc. Rev.*, 2010, vol. 39, no. 6, p. 1986.
22. Li, J.R., Yu, Q., Tao, Y., et al., *Chem. Commun.*, 2007, no. 22, p. 2290.
23. Lloret, F., Julve, M., Cano, J., et al., *Inorg. Chim. Acta*, 2008, vol. 361, nos. 12–13, p. 3432.

Translated by E. Yablonskaya